Role for P2X Receptors in Long-Term Potentiation

Yuri V. Pankratov, Ulyana V. Lalo, and Oleg A. Krishtal

Department of Cellular Membranology, Bogomoletz Institute of Physiology, 01024 Kiev, Ukraine

ATP receptors participate in synaptic transmission and intracellular calcium signaling in the hippocampus by providing a component of the excitatory input to CA1 pyramidal neurons. The activation of P2X purinoreceptors generates calcium influx that does not require cell depolarization, but this response desensitizes at increased rates of stimulation. Here we show that inhibition of P2X receptors dramatically facilitates the induction of long-term potentiation (LTP). High-frequency stimulation (HFS) (1 sec) induced LTP in CA1, whereas brief HFS (0.2 sec) caused only short-term potentiation. However, when P2X receptors were inhibited by PPADS (pyridoxal phosphate-6-azophenyl-2′-4′-disulphonic acid) or desensitized by the non-hydrolyzable ATP analog α,β-methyleneATP, brief HFS reliably induced LTP. Inhibition of P2X receptors had no facilitatory effect on LTP when NMDA receptors were blocked. We hypothesized that P2X receptors affect the threshold for LTP by altering Ca^{2+}-dependent inactivation of NMDA receptors. In isolated pyramidal CA1 neurons and hippocampal slices, activation of P2X receptors did cause inhibition of NMDA receptor-mediated current. We suggest that, by controlling the background calcium and thus the activity of NMDA receptors at low firing frequencies, P2X receptors act as a dynamic low-frequency filter so that weak stimuli do not induce LTP.

Key words: P2X receptors; long-term potentiation; NMDA receptor inactivation; α,β-methyleneATP; PPADS; CA1 neurons

The activity-dependent phenomenon long-term potentiation (LTP) provides excitatory synapses with Hebbian properties and may serve as the basis of learning and memory. High-frequency stimulation (HFS) leads to LTP in hippocampal CA3–CA1 synapses because it allows postsynaptic NMDA receptors to create a powerful calcium signal in dendritic spines of depolarized pyramidal neurons. The level of intracellular calcium determines whether the efficacy of synaptic connections is enhanced or depressed (Artola and Singer, 1993; Debanne and Thompson, 1994; Malenka and Nicoll, 1999). Previously, NMDA receptors and voltage-gated Ca channels have been considered as the main source of calcium influx, particularly for CA1 hippocampal neurons. However, a role for a purinergic component of synaptic transmission has been demonstrated recently (Pankratov et al., 1999). ATP is released from nerve endings (Illes and Nurenberg, 1993; Zimmermann, 1994; Cunha et al., 1996), and ATP receptors show a widespread distribution in the brain (Balcar et al., 1995; Collo et al., 1996; Seguela et al., 1996). ATP acting at P2X receptors mediates synaptic transmission in the medial habenula (Edwards et al., 1992) and hippocampus (Pankratov et al., 1998). Nevertheless, the specific physiological role of ATP receptors in the CNS remains unclear. The effects of ATP are mediated by ionotropic (P2X) and metabotropic (P2Y) purinoreceptors. The former depolarizes neurons and has a considerable calcium permeability (Buell et al., 1996; Edwards et al., 1997; Virginio et al., 1998), whereas the latter controls calcium release from intracellular stores (Harden et al., 1995; Ralevic and Burnstock, 1998). The entry of calcium through purinoreceptor-operated channels become larger with more negative membrane voltage in contrast to NMDA receptors for which calcium entry requires membrane depolarization. Thus, the purinergic component of synaptic transmission may increase intracellular calcium when the membrane potential is near its resting level. Correspondingly, the role of ionotropic purinergic component in the calcium signaling and synaptic plasticity may be quite different from the function of NMDA receptors. Here we show that inhibition of P2X receptors facilitates the induction of LTP.

MATERIALS AND METHODS

Hippocampal slices. Experiments were performed on transverse 200- to 400-μm-thick hippocampal slices of Wistar rats (19- to -21-d-old animals). The brain was rapidly removed after decapitation and placed into ice-cold artificial CSF (ACSF) containing the following (in mM): 130 NaCl, 3 KCl, 1 MgCl$_2$, 2 CaCl$_2$, 1 NaH$_2$PO$_4$, 26 NaHCO$_3$, and 15 glucose (gassed with 95% O$_2$–5% CO$_2$ to obtain a final pH of 7.4). After dissection, slices were placed in a holding chamber in which they were maintained at room temperature (22–24°C) for 3–6 hr until they were placed in the recording chamber, also at room temperature. During incubation and recording, slices were kept in ASCF of the following composition (in mM): 135 NaCl, 2 KCl, 2 CaCl$_2$, 1.0 MgCl$_2$, 1 NaH$_2$PO$_4$, 26 NaHCO$_3$, and 15 glucose (gassed with 95% O$_2$–5% CO$_2$ to obtain a final pH of 7.4).

Electrophysiological recordings. Using an RK-400 amplifier (Bio-Logic, Claix, France), the EPSCs were recorded in the conventional whole-cell configuration with the patch pipette (2–5 MΩ) filled with the following intracellular solution containing (in mM): 80 K$_2$HPO$_4$, 20 KCl, and 10 HEPES, pH 7.3 ("phosphate" solution). Two solutions were also used to test the role of intracellular calcium in the observed phenomena (in mM): 110 CsCl, 10 NaCl, 10 HEPES, pH 7.3, 2 MgATP, and 0.1 EGTA ("CsCl 0.1 mM EGTA" solution); and 110 CsCl, 10 NaCl, 10 HEPES, pH 7.3, 2 MgATP, 1 CaCl$_2$, and 10 EGTA ("CsCl 10 mM EGTA" solution). The series and the input resistances were 7 $\pm$ 3 and 300 $\pm$ 150 MΩ, respectively, and varied for <20% in the cells accepted for analysis. All of the recordings of excitatory synaptic currents were made in the presence of 100 μM picrotoxin in the superfusing solution. The field EPSPs were recorded from the stratum radiatum of area CA1 using glass microelectrodes filled with ACSF (impedance, 1–2 MΩ). The Schaffer collateral–commissural pathway was stimulated with a 50-μm-thick Ni–Cr bipolar electrode positioned on the slice surface in the stratum

radiatum. Stimulus intensity was adjusted to evoke EPSPs at ~30–40% of the maximal response.

[Ca²⁺]ᵢ measurement. The hippocampal neurons were loaded with the calcium indicator fura-2 by a 25-min-long incubation of the hippocampal slices in the ACSF supplemented with fura-2 AM (10 μM) and pluronic F-127 detergent (0.02%) at 35°C. For the period of dye loading, slices were kept under a controlled air environment (5% CO_2–95% O_2). Subsequently, the slices were incubated in ACSF for an additional 40 min to ensure fura-2 AM deetherification. For fura-2 excitation, cells were illuminated at a wavelength of 390 nm. The emitted light was collected at 530 ± 10 nm by a photomultiplier controlled by a fura-2 Data Acquisition System (Luigs & Neumann, Ratingen, Germany) and a TIDA interface (Heka Electronik, Lambrecht/Pfalz, Germany). To reduce the background fluorescence and select the region of interest, the UV illumination was attenuated by an adjustable diaphragm installed in the light path. Dye-loaded neurons were positioned in such a way that the fluorescent signal was collected from their somata. Relative changes in the $[Ca^{2+}]_i$ were quantified as changes in F/F_0, where F_0 and F are the fluorescence before and during neuronal activity (corrected for bleaching during recording). The bleaching was corrected by measuring the fluorescence in the neuron without stimulation. Tissue autofluorescence was subtracted after the measurement of fluorescence at a parallel location in the slice away from the dye-filled cell.

Acutely isolated pyramidal neurons. After dissection, hippocampal slices were placed in the ACSF supplemented with 0.8 mg/ml trypsin (type XI; Sigma, St. Louis, MO) and incubated at 32°C for 20 min. After that, the slices were rinsed of the enzyme and maintained at room temperature (22–24°C) for 4–6 hr. Single CA1 neurons were isolated by successive triturating through several pipettes with opening diameters from 0.5 to 0.1 mm. After dissociation, neurons were placed in the extracellular solution containing the following (in mM): 150 NaCl, 5 KCl, 2 CaCl₂, 1 MgCl₂, and 10 HEPES, pH 7.3. The cells were suitable for recording within 2–3 hr. Only cells of characteristic pyramidal shape were used for the experiments. Whole-cell conventional patch-clamp recordings were performed by using the patch pipette (2–4 MΩ) filled with the following intracellular solution (in mM): 120 CsCl, 10 NaCl, 10 HEPES, 2 MgATP, and 0.1 EGTA, pH 7.3. The series and input resistance were 6 ± 2 and 800 ± 200 MΩ, respectively.

Drug application. A modified "square-pulse" concentration clamp method (Pankratov et al., 2001) was used for the rapid 200-msec-long application of agonist containing solutions with immediate washout. The tip of the recording pipette, attached to a neuron, was inserted into a glass tube (1 mm inner diameter) through a tiny opening (0.6 mm inner diameter). The lower end of the tube was submerged into the external solution in the chamber. The upper end of the tube was connected via the V-shaped plastic tube and computer-controlled valves to the sources of negative and positive pressures allowing the suction of drug-containing solution or backward washout with clear extracellular solution.

To examine the Ca²⁺ signals in pyramidal cells, ATP or α,β-methyleneATP (α,β-meATP) (100 μM) were applied by pressure ejection (5–10 kPa) from a pipette with a 200–300 μm internal diameter The pressure was switched by a solenoid valve controlled by computer. The pipette was positioned perpendicularly to the flow of the bath perfusing solution near the edge of stratum radiatum. The agonist was applied in the presence of 10 μM (2,3-dioxo-6-nitro-1,2,3,4-tetrahydro-benzo[f]quinoxaline-7-)sulfonamide (NBQX) and 50 μM 2-amino-5-phosphovaleric acid (D-APV) at 5 min intervals using 10 sec pulses.

Data analysis. All data are expressed as mean ± SD. The statistical analysis was performed using Origin 6.0 software (Microcal Software, Northampton, MA). The standard paired *t* test was used for analysis of changes in the EPSP, and linear regression analysis was used to estimate the relationship between inactivation of NMDA receptors and P2X receptor-mediated current. The significance level of linear correlation was evaluated as probability, *p*, of null hypothesis, H_0, as defined by *F* test.

Materials. The following compounds were purchased from Tocris Cookson (Bristol, UK): NBQX, D-APV, and pyridoxal phosphate-6-azophenyl-2′-4′-disulfonic acid (PPADS). Fura-2 AM was delivered by Molecular Probes (Eugene, OR). All other chemicals were from Sigma.

RESULTS

Figure 1 shows that, with low-frequency stimulation of the Schaffer collaterals, a small fraction of the fast EPSC recorded in CA1 cells is mediated by ATP. After blocking glutamate receptors with NBQX and D-APV, the residual component can be inhibited
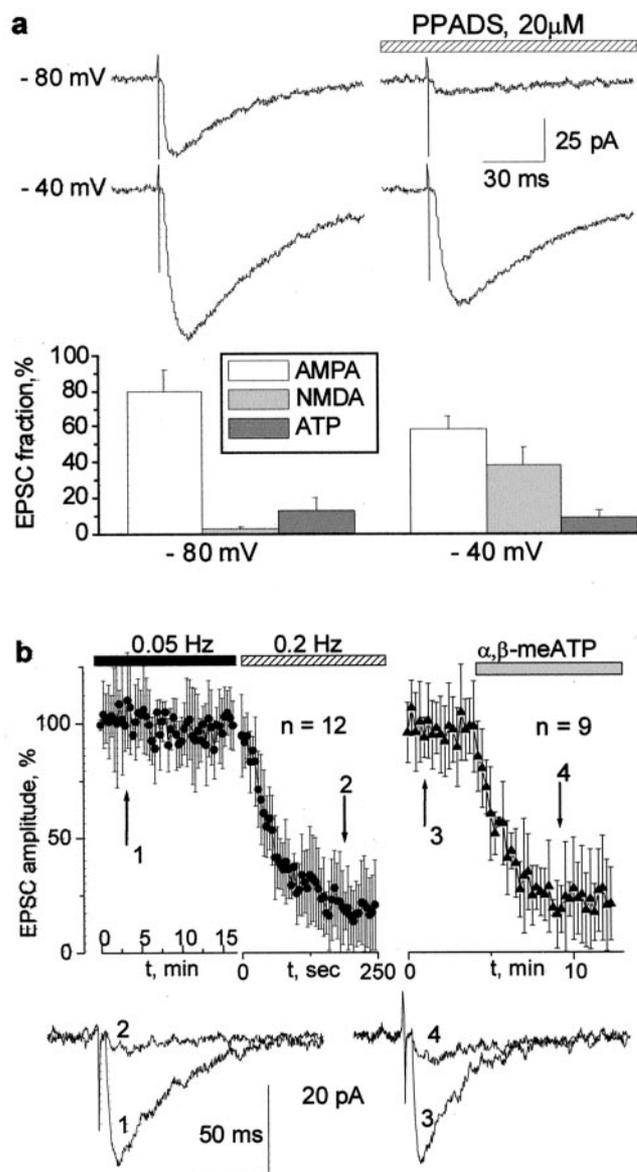

Figure 1. Purinergic synaptic input in hippocampal CA1 neurons. *a*, EPSCs elicited by stimulation of the Schaffer collaterals. The current was measured at two membrane voltages always in the presence of NBQX (10 μM). *Right column*, Application of PPADS (20 μM) on the background of NBQX. Each *trace* is the average of five consecutive responses. Note that, at a holding potential of −80 mV, the EPSC consists almost entirely of P2X-mediated current. *Bottom diagrams* demonstrate the relative contribution of the AMPA, NMDA, and ATP receptor-mediated currents to the total EPSC. Each *column* represents the mean ± SD for 15 cells. *b*, The desensitization of the ATP-mediated EPSC, measured in the presence of NBQX (10 μM) and D-APV (50 μM) at a holding voltage of −75 mV. The *top left graph* demonstrates that the amplitude of the purinergic component of the EPSC in CA1 neurons is stable when the frequency of stimulation is 0.05 Hz but quickly fades when the frequency is increased to 0.2 Hz. The *top right graph* demonstrates the disappearance of the purinergic component of the EPSC after bath application of 20 μM α,β-meATP, a nonhydrolyzable analog of ATP, with stimulation frequency of 0.05 Hz. The representative current traces obtained at the times indicated by the *arrows* are demonstrated below the graphs.

by 20 μM PPADS (55 ± 25%; *n* = 20). This ATP-mediated component comprised 5–20% of the total synaptic current depending on the holding potential. With AMPA receptors only blocked, the residual postsynaptic current at −80 mV is almost
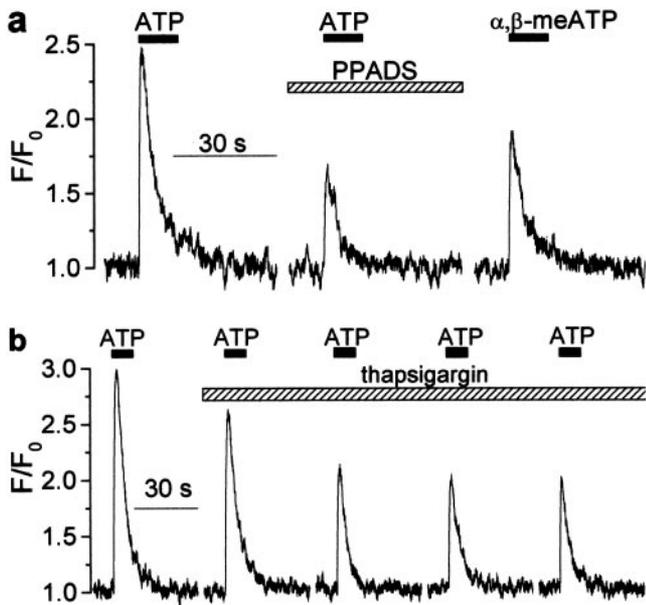
Figure 2. ATP-induced $[Ca^{2+}]_i$ transients in CA1 pyramidal neurons. *a*, Examples of $[Ca^{2+}]_i$ transients induced in the pyramidal cells by fast application of ATP (100 μM) and α,β-methyleneATP (100 μM) to the hippocampal slice in control and after bath application of 20 μM PPADS. All *traces* were recorded in one and the same cell at 5 min intervals. Note the substantial amplitude of the response to α,β-methyleneATP, which is only attributable to the calcium influx via ionotropic ATP-receptors. *b*, Examples of $[Ca^{2+}]_i$ transients induced by repetitive fast application of ATP (100 μM) in the presence of 1 μM thapsigargin at 5 min time intervals. It is worth noting that the amplitudes of the third and the following transients, which are attributable to entry of the extracellular calcium via ionotropic ATP receptors, comprise ~40% of the initial response, which represents the combined activity of P2X and P2Y purinoreceptors.

completely purinergic. At −40 mV, the purinergic component is approximately one-fifth of the NMDA component. The purinergic component of the EPSC declined steeply when the stimulation frequency was increased to 0.2 Hz (Fig. 1*b*). A similar effect was seen by applying 20 μM α,β-meATP, a nonhydrolyzable ATP receptor agonist (Buell et al., 1996), and we ascribe the disappearance of the purinergic component to the desensitization, which is commonly observed for P2X receptors. It should be noted that the effects of PPADS and α,β-meATP, as well as the rate of desensitization of the ATP-mediated EPSCs, showed large cell to cell variations. A small fraction of the current (5–25%) persists after application of PPADS and repeated episodes of high-frequency stimulation. This variability is most probably attributable to the differential expression of several P2X receptor subtypes, presumably P2X3, P2X4, and P2X6, as well as their heteromers (Seguela et al., 1996; Ralevic and Burnstock, 1998). These receptors have different sensitivity to PPADS and α,β-meATP, as well as different desensitization kinetics.

We measured $[Ca^{2+}]_i$ transients evoked in CA1 pyramidal cells by fast application of 100 μM ATP to hippocampal slices (Fig. 2). Prominent signals were observed in 20 of 25 cells, and these were inhibited by 45 ± 25% in the presence of PPADS (20 μM; $n = 12$). They were unaffected by 1 μM tetrodotoxin and/or glutamate receptor blockers. α,β-meATP at the concentration of 100 μM also evoked calcium transients in 17 of 22 cells (30–60% of the amplitude of those caused by ATP). α,β-meATP does not activate P2Y receptors (Ralevic and Burnstock, 1998), so this experiment indicates that a substantial fraction of the rise in $[Ca^{2+}]_i$ results

from influx through P2X receptors. Blocking of refilling of the intracellular Ca^{2+} stores by thapsigargin (Lytton et al., 1991) decreased the calcium signal, indicating some contribution of the metabotropic signal and/or Ca^{2+}-induced Ca^{2+} release (Fig. 2*b*). However, a substantial residual component remained (50 ± 15%; $n = 6$), demonstrating a substantial ionotropic P2X receptor-mediated component.

An increase in postsynaptic calcium is widely believed to play a key role in synaptic plasticity (Bliss and Collingridge, 1993; Cummings et al., 1996; Malenka and Nicoll, 1999). The purinergic component of the EPSC might play an important role in long-term plasticity because the P2X-receptor mediated calcium entry would progressively increase with hyperpolarization. This is in contrast to the activation of NMDA receptors, in which current decreases with hyperpolarization beyond approximately −40 mV. We elicited LTP at CA3–CA1 synapses according to established protocols and measured it as the slope of the field EPSP. In control conditions, high-frequency stimulation (100 Hz, 1 sec) increased the slope by 125 ± 45%, and this increase persisted for up to 3 hr (Fig. 3*a*). A train of 100 Hz for 0.2 sec did not cause LTP, even when the train was repeated (Fig. 3*b*). However, in the presence of the P2X receptor blocker PPADS (20 μM), even the short train evoked substantial LTP (Fig. 3*b*). The field EPSP slope increased by 69 ± 34% at 1 hr, and this effect was highly significant ($n = 15$; $p < 0.01$; Student's t test).

The question arises whether the observed phenomenon is attributable to the presynaptic or postsynaptic action(s) of PPADS. This substance blocks both P2X and P2Y receptors (Buell et al., 1996). Metabotropic P2Y receptors are known to downregulate transmitter release by partial inhibition of Ca channels (Ralevic and Burnstock, 1998). Correspondingly, PPADS might enhance synaptic transmission via a presynaptic mechanism. In fact, we observed a small increase in the field EPSP in the presence of PPADS. The effect reached 6 ± 4% for the mean amplitude and 8 ± 6% for the coefficient of variation ($n = 15$). This minor effect does not seem to be capable of causing a profound facilitation of LTP, but we further addressed the problem by using α,β-meATP as a desensitizing agonist, which is selective for P2X receptors (Ralevic and Burnstock, 1998). This substance did not increase the amplitude of EPSP but completely reproduced the effect of PPADS: LTP could be elicited by a 0.2 sec stimulus train in the presence of 20 μM α,β-meATP (Fig. 3*c*), and the slope of the field EPSP was increased by 45 ± 22% at 1 hr ($n = 10$; $p < 0.02$; Student's t test).

These results imply that the observed facilitation of LTP induction is predominantly related to the inhibition of the ionotropic P2X receptors. The experiments on isolated pyramidal neurons (see below) suggest that the affected P2X receptors are postsynaptic.

The LTP at the CA1 synapse is NMDA receptor dependent (Bliss and Collingridge, 1993; Cummings et al., 1996). We checked whether the role of NMDA receptors in LTP induction remained crucial under conditions of inhibited P2X receptors. Figure 4*a* shows that, in the presence of D-APV, high-frequency stimulation induces only brief potentiation, followed by a modest long-term depression (LTD) of the field EPSP. This effect is reversible, and, after removing D-APV from the bath solution, LTP can be induced. The conversion of the effect of brief tetanic stimulation from LTP to LTD as a result of NMDA receptor inhibition has been reported previously (Cummings et al., 1996). PPADS did not alter this phenomenon, confirming that the intrinsic properties of LTP induction were similar. Under simultaneous action of D-APV and PPADS, 1 sec HFS induced depres-
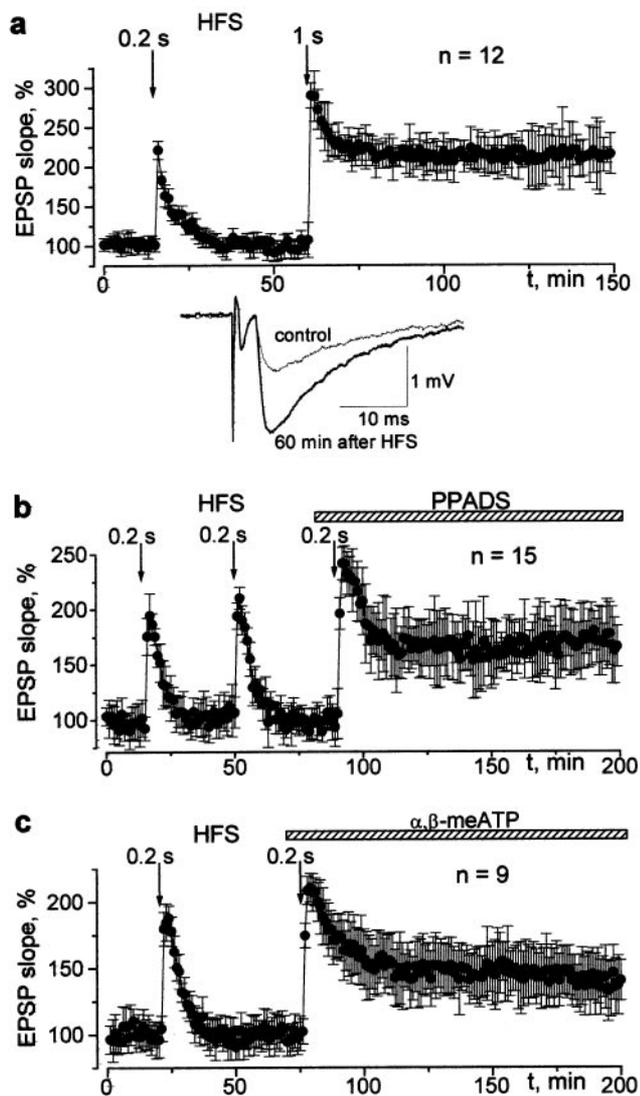
Figure 3. The changes in the CA1 field potentials induced by 100 Hz stimulation delivered to the Schaffer collateral in the control and after inhibition of the ATP receptors. *a,* The time course of the potentiation evoked by 0.2 and 1 sec of 100 Hz stimulation trains in control conditions. Examples of field EPSPs recorded before and 60 min after the 1-sec-long HFS train are indicated in the *inset.* Each *trace* represents the average of 10 EPSPs. *b, c,* The time course and magnitude of the potentiation evoked by the 0.2 sec HFS train in control and after bath application of 20 μM PPADS and α,β-methyleneATP, respectively. Baseline stimulation frequency is 0.08 Hz.
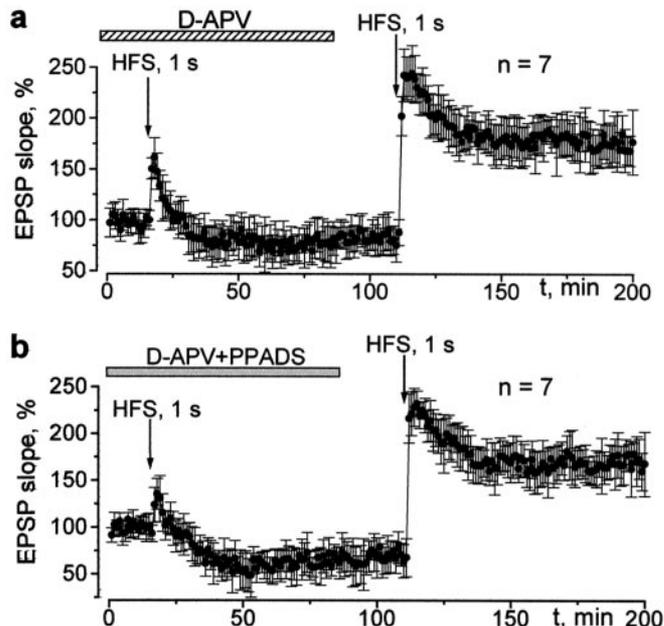

Figure 4. Inhibition of purinoreceptors does not affect the "NMDA paradigm." The changes in the field EPSP slope evoked by the 1 sec HFS train after bath application of 25 μM D-APV (*a*) and simultaneous application of 25 μM D-APV and 20 μM PPADS (*b*). The inhibition of NMDA receptors reversibly blocks the induction of LTP independently of the activity of P2X receptors. Baseline stimulation frequency is 0.08 Hz.

sion instead of potentiation, but, during washout of D-APV, the 0.2 sec HFS train induced LTP (Fig. 4*b*). These observations provide support for the hypothesis that the direction of the change in synaptic transmission depends on the level of the activity-dependent rise in $[Ca^{2+}]_i$ (Malenka and Nicoll, 1999; Luscher et al., 2000).

The above results suggest that ATP, coreleased with glutamate, causes an inhibition of LTP at low frequencies of background tonic stimulation. At higher frequencies of background stimulation, ATP loses its postsynaptic action attributable to desensitization of P2X receptors. One mechanism by which P2X receptors might affect the machinery of LTP could be through the Ca^{2+}-dependent inactivation of NMDA-mediated responses (Rosenmund et al., 1995; Kyrozis et al., 1996). This hypothesis was tested,

and the results are shown in Figure 5. The Schaffer collaterals were continuously stimulated in the presence of NBQX. The current measured at -40 mV represented the NMDA component of the EPSC, whereas an exclusively purinergic component was present at -80 mV (compare with Fig. 1*a*). The NMDA component was strongly inhibited after each episode of low-frequency stimulation at -80 mV (Fig. 5*a*). The gradual recovery of NMDA current during the stimulation at -40 mV is incomplete because of the calcium influx via NMDA receptor-operated channels. However, after a period without stimulation, the amplitude of NMDA receptor-mediated EPSC completely recovered (Fig. 5*a*). As already reported (Rosenmund et al., 1995; Kyrozis et al., 1996), NMDA receptors recover from inactivation when the calcium concentration falls back to resting levels. The inhibition of NMDA component was abolished by PPADS, suggesting that NMDA receptors were inhibited by the activity of P2X receptors (Fig. 5*a*).

The inhibition of the NMDA component of the EPSC appears to be dependent on the calcium buffering capacity of the intracellular solution. Three compositions of intracellular solution were tested: one containing K_2HPO_4 (phosphate solution) and two CsCl-based solutions, with the solution with 10 mM EGTA providing very strong buffering of Ca^{2+} and the solution with 0.1 mM of EGTA allowing large variations in the intracellular Ca^{2+} concentration. These solutions may be ranked according to their potency as Ca^{2+} buffers from higher to lower: 10 mM EGTA solution, phosphate solution, and 0.1 mM EGTA solution. The inhibitory effect was evaluated as the difference in the steady level of amplitude of NMDA current before and after stimulation at -80 mV. We did not observe the inhibition of NMDA currents in all of the cells perfused with 10 mM EGTA ($n = 10$). As to the cells perfused with 0.1 mM EGTA ($n = 15$), the inhibition of NMDA current was even larger than in the case of the phosphate solution (Fig. 5*b*).
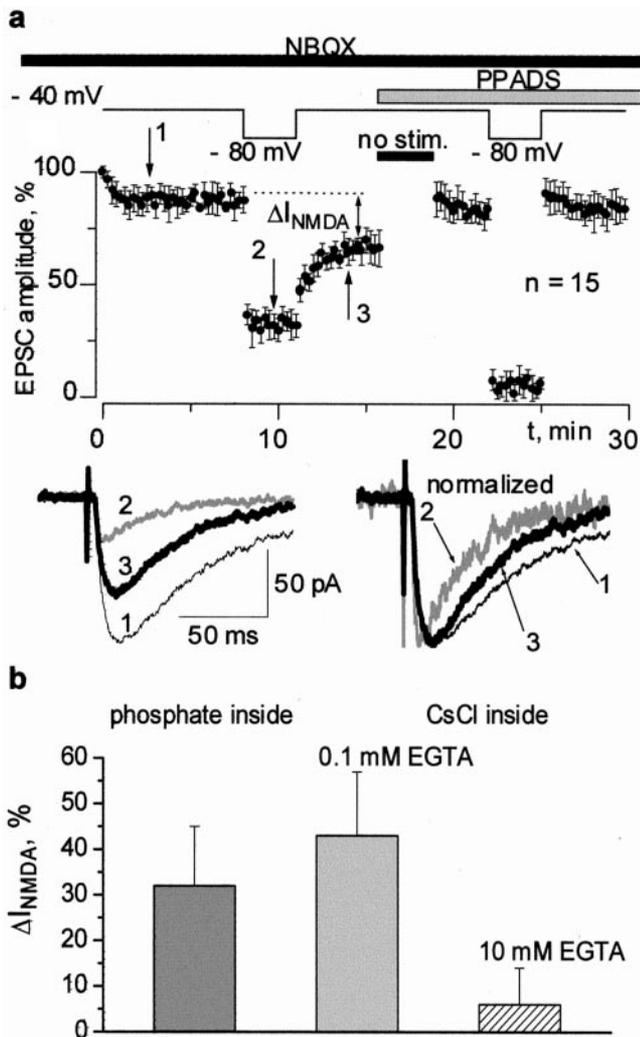
Figure 5. NMDA component of EPSC is inactivated by low-frequency stimulation at a strongly negative voltage. This effect is inhibited by PPADS and depends on the Ca^{2+}-buffering capacity of the intracellular saline. *a*, EPSCs comprising NMDA and purinergic components were continuously recorded at two membrane potentials, first at −40 mV (practically pure NMDA component) and then at −80 mV (only the purinergic component is responsible for the measured inward current). Note a substantial inhibition of the NMDA component after return of the voltage to −40 mV (the EPSCs measured at the moments indicated by the *numbers* are demonstrated in the *inset*, and each *trace* is the average of 5 EPSCs). The kinetics of the EPSC recorded again at −40 mV become faster because of the decrease in the NMDA receptor-mediated fraction. Application of PPADS (20 μM) to the same cell leads to the complete disappearance of this effect. *b*, A decrease in the NMDA receptor-mediated component of EPSC (ΔI_{NMDA}) has been measured as shown in *a* using different compositions of intracellular solution (see Materials and Methods). The buffering of intracellular calcium by 10 mM EGTA prevents the inactivation of NMDA receptors.

So, the stronger the buffering of intracellular Ca^{2+} was, the weaker was the inhibition of NMDA currents observed after a period of low-frequency stimulation at strongly negative membrane voltages. The inhibition of NMDA receptors could also be prevented by the purinergic antagonist PPADS. The above results suggest that Ca^{2+} influx mediated by purinoreceptors may bring a contribution in the inactivation of NMDA receptors. To obtain direct evidence of interaction between P2X and NMDA receptors, we performed experiments on dissociated pyramidal CA1

neurons. The inward currents evoked by application of ATP were observed in 19 of 24 cells tested. The amplitude of the response to 20 μM ATP was in the range of 20–120 pA at a holding potential of −80 mV. The mean density of ATP-induced current was 4 ± 2 pA/pF. The decay of current had biexponential kinetics with time constants of 28 ± 8 and 850 ± 150 msec, with the ratio of fast to slow components measuring 0.44 ± 0.25. These observations are consistent with the participation of different P2X receptor subtypes. All of the tested cells demonstrated a response to NMDA whose amplitude (200–300 pA) was stable during repetitive application of agonist at 2 min intervals. The amplitude of current evoked by the application of 30 μM NMDA at −40 mV was typically two to three times higher than the amplitude of the response to 20 μM ATP at −80 mV.

When the response to NMDA was evoked in a few seconds after a short (200 msec) application of ATP, the amplitude of NMDA current did not alter significantly. At the same time, when ATP was applied for a much longer time (10 sec) at a holding potential of −80 mV, the amplitude of the NMDA response decreased considerably (Fig. 6*a*). The larger the response to ATP was, the higher was the decrease in the amplitude of NMDA receptor-mediated current. On the other hand, the inhibition of NMDA receptors was not observed in the cells that did not respond to ATP. The dependence of decrease in the amplitude of response to NMDA (I_{NMDA}) on the relative amplitude of P2X receptor-mediated current (I_{P2X}/I_{NMDA}) is shown in Figure 6*b*.

The 10-sec-long preapplication of α,β-meATP (20 μM) also inhibited the NMDA current (Fig. 6*b*), indicating that this effect is mediated predominantly by ionotropic P2X receptors. Moreover, the inhibitory effect of both P2X receptor agonists correlated with the amplitude of the ATP-evoked current (Fig. 6*b*). The linear regression analysis gave the correlation coefficient $R > 0.7$ with a significance level $p < 0.01$, indicating toward the strong modulatory effect of ATP receptors.

For several cells, although they demonstrated a relatively small response to ATP, the inhibition of NMDA receptor-mediated currents by preapplication of ATP was very high, whereas such a deviation from the main correlation was not observed for α,β-meATP. This fact implies that metabotropic P2Y receptors may also contribute to the rise in intracellular calcium and subsequent inhibition of NMDA receptors.

To prove the role of calcium in the inactivation of NMDA receptors, we reproduced the same protocol after substitution of extracellular calcium for barium. As shown in Figure 6*c*, application of ATP failed to induce NMDA receptor inactivation in the absence of calcium ions in the extracellular medium. Hence, the influx of calcium through P2X receptor channels is crucial for ATP-induced inactivation of NMDA receptors.

DISCUSSION

Our data demonstrate that ATP receptors mediate a minor component of excitatory synaptic current and participate in the intracellular calcium signaling in CA1 pyramidal neurons. Although P2X receptor-mediated synaptic input is small compared with the AMPA component, it may play an important role, providing a calcium influx at low membrane potentials when NMDA receptors are not active. Another important feature of purinergic synaptic current is its tendency to desensitization with increased stimulation frequency. Similar behavior was reported for purinergic EPSC in the medial habenula (Edwards et al., 1997), in which the number of failures increased at higher stimulation frequencies. The decline of purinergic EPSC may be related to the
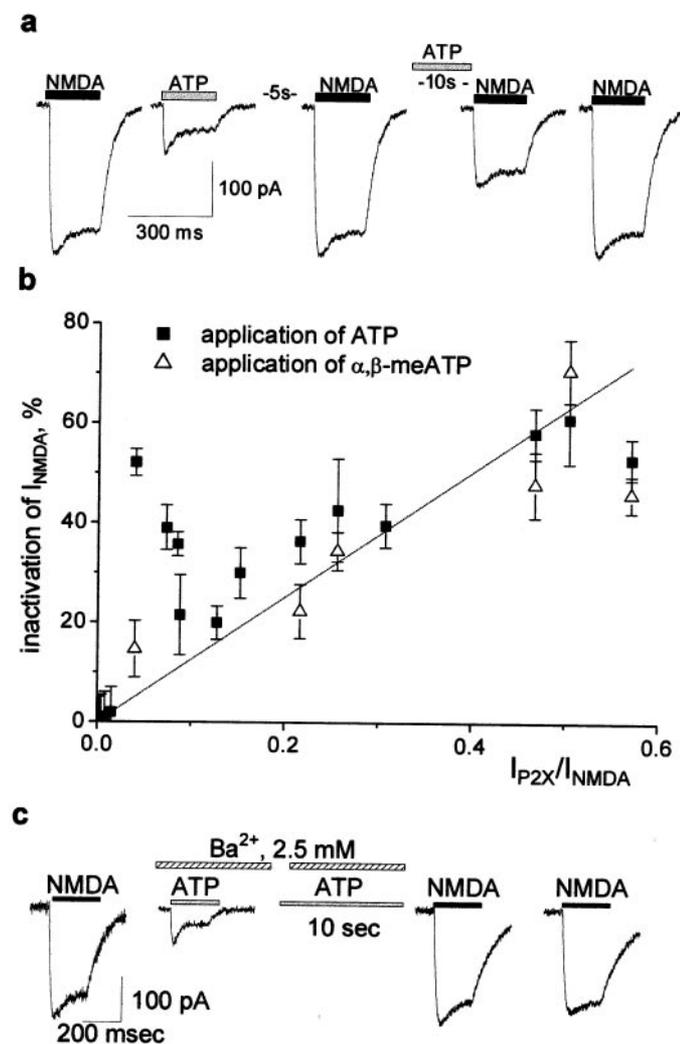
Figure 6. Interaction between P2X and NMDA receptors in acutely isolated CA1 pyramidal neurons. *a*, examples of inward currents evoked by short (200 msec) applications of NMDA and ATP. The *traces* represent (from *left* to *right*) the control response to NMDA, the response to ATP, the control response to NMDA evoked 5 sec after a 200 msec application of ATP, the response to NMDA evoked after a 10 sec preapplication of ATP, and the control response to NMDA. *b*, Inhibition of NMDA receptors correlates with the amplitude of response to ATP. The relative decrease in the amplitude of NMDA-evoked current (I_{NMDA}) caused by 10-sec-long application of P2X agonists (ATP, 20 μM, *filled squares*; α,β-methyleneATP, 20 μM, *open triangles*) is plotted against the ratio of current mediated by P2X receptors to the current mediated by NMDA receptors (I_{P2X}/I_{NMDA}). Each *point* represents a single cell tested. The inhibition of NMDA receptors is higher for the cells exhibiting larger P2X receptors-mediated currents. The inhibition did not occur in the cells that did not exhibit the response to ATP. Several exclusions observed under ATP, but not α,β-methyleneATP, can be tentatively attributed to the activity of P2Y receptors in those particular three cells. The *dotted line* represents the result of linear regression analysis. A high (correlation coefficient, $R = 0.72$) and significant ($p < 0.01$) correlation shows that ATP receptors can strongly influence the NMDA receptors. *c*, Substitution of calcium in the extracellular solution for barium eliminates the ATP-induced inactivation of NMDA receptors. The *traces* represent (from *left* to *right*) the control response to NMDA, the response to ATP after substitution of extracellular Ca^{2+} for Ba^{2+}, the response to NMDA evoked after a 10 sec preapplication of ATP in the Ba^{2+}-containing medium, and the control response to NMDA. NMDA (30 μM) was applied on the background of 10 μM glycine at a holding potential of -40 mV; ATP (20 μM) was applied at -80 mV. Intracellular solution contained 0.1 mM EGTA.

desensitization of postsynaptic P2X receptors, as well as down-regulation of synaptic transmission by extracellular ATP via pre-synaptic P2Y purinoreceptors (Koizumi et al., 1997; Ralevic and Burnstock, 1998). Although presynaptic P2Y receptors may play a certain role in the synaptic plasticity, the effect of LTP facilitation observed in the present paper should be attributed mainly to P2X receptors, because a similar effect may result from the desensitization of P2X receptors by their selective agonist α,β-meATP.

The role of P2X receptors is supported by data on the interaction between ATP- and NMDA-induced current. The observation of ATP-induced currents in the pyramidal neurons is important in itself as direct evidence of the presence of functional P2X receptors. The percentage of cells that do not exhibit ATP-induced currents and calcium transients (20–25%) is very close indeed to the percentage of failures in the observation of purinergic EPSCs (Pankratov et al., 1998). On the other hand, the variability of the P2X-mediated response recorded in the somata of isolated cells (Fig. 6*b*) is higher than the variability of synaptic current mediated by dendritic P2X receptors. So one could suggest the different levels of P2X receptor expression in the soma and dendrites of pyramidal neurons. Our results imply that, in at least 75–80% of pyramidal neurons, activity of P2X receptors may cause Ca^{2+}-dependent inactivation of NMDA receptors. It is not an unique example of interaction between P2X and other ligand-gated receptor channels. The cross-inhibition between P2X and nicotinic acetylcholine receptors has also been widely reported (Nakazawa, 1994; Zhou and Galligan, 1998; Khakh et al., 2000). The mechanism of this effect seems to be different from inactivation of NMDA receptors. It has been demonstrated that interaction between purinergic and cholinergic receptors is Ca^{2+} independent (Zhou and Galligan, 1998) and presumably related to the spread of conformational changes from one receptor to its neighbor (Khakh et al., 2000).

The presented data indicate that the synaptic stimulation of P2X receptors determines the level of activity of NMDA receptors by regulating dynamic equilibrium between periodical Ca^{2+} transients and mechanisms that bring Ca^{2+} concentration back to the resting levels. The level of intracellular Ca^{2+} is known to change the efficacy of synaptic connections in opposing ways by regulating phosphorylation and dephosphorylation. One of the most widely accepted views is that a moderate rise in the intracellular Ca^{2+} concentration should lead to the activation of phosphatases and cause LTD, whereas a larger rise in $[Ca^{2+}]_i$ causes the activation of kinases, primarily of Ca^{2+}/calmodulin-dependent (CaM) kinase, subsequently leading to LTP. CaM kinase undergoes autophosphorylation and may remain active even after the return of $[Ca^{2+}]_i$ to basal level. However, its opposing phosphatase has a 25–100 times higher affinity for calcium and can dephosphorylate the autophosphorylated kinase (Debanne and Thompson, 1994). Competition between these mechanisms provides the threshold for bi-directional long-lasting changes of synaptic connections. Two mutually nonexclusive hypotheses of the expression of synaptic plasticity are most widely accepted: (1) direct upregulation and downregulation of AMPA receptors (Malenka and Nicoll, 1999) and (2) morphological changes in the dendritic spines (Edwards, 1995; Luscher et al., 2000). Both hypotheses account for bi-directional changes in synaptic efficacy directed by the activity of phosphatases and kinases.

Our results on the participation of P2X receptors in synaptic plasticity are in good agreement with the paradigm concerning the earlier phase of the LTP induction. Thus, in the vicinity of resting potential (that is, during the intervals between spikes or

bursts), purinergic synaptic input may serve as the main source of intracellular calcium (Zimmermann, 1994; Cunha et al., 1996). This background calcium influx maintains the tonic activity of phosphatases and determines the efficiency of the subsequent episode of activity for the induction of LTP. In the course of such episodes, NMDA receptors available for activation in a given neuron have to create a sufficient calcium signal. The efficiency of NMDA receptors is determined, among other factors, by the level of calcium-dependent inactivation (Rosenmund et al., 1995). It appears that P2X receptors strongly influence the basal level of calcium-dependent inactivation of NMDA receptors and correspondingly determine the threshold for the induction of LTP.

In summary, our results indicate that ATP coreleased with glutamate allows calcium to enter the postsynaptic cell and thereby inhibits the effectiveness of NMDA receptors in the induction of LTP. P2X receptors bring their contribution to synaptic transmission mainly at low frequencies of stimulation and low membrane potential. In other words, they act as a dynamic low-frequency filter, preventing weak stimuli from inducing long-lasting changes in synaptic efficacy.

REFERENCES

Artola A, Singer W (1993) Long-term depression of excitatory synaptic transmission and its relationship to long-term potentiation. Trends Neurosci 18:41–48.

Balcar VJ, Li Y, Killinger S, Bennett MR (1995) Autoradiography of P2X ATP receptors in the rat brain. Br J Pharmacol 115:302–306.

Bliss TVP, Collingridge GL (1993) A synaptic model of memory: long-term potentiation in the hippocampus. Nature 361:31–39.

Buell G, Collo G, Rassendren F (1996) P2X receptors: an emerging channel family. Eur J Neurosci 8:2221–2228.

Collo G, North RA, Kawashima E, Merlo-Pich E, Neidhart S, Surprenant A, Buell G (1996) Cloning of P2X5 and P2X6 receptors and the distributions and properties of an extended family of ATP-gated ion channels. J Neurosci 16:2495–2507.

Cummings JA, Mulkey RM, Nicoll RA, Malenka RC (1996) Ca^{2+} signaling requirements for long-term depression in the hippocampus. Neuron 16:825–833.

Cunha RA, Vizi SE, Ribeiro AJ, Sebastiao AM (1996) Preferential release of ATP and its extracellular catabolism as a source of adenosine upon high- but not low-frequency stimulation of rat hippocampal slices. J Neurochem 67:2180–2187.

Debanne D, Thompson SM (1994) Calcium: a trigger for long-term depression and potentiation in the hippocampus. News Physiol Sci 9:257–260.

Edwards FA (1995) LTP—a structural model to explain the inconsistencies. Trends Neurosci 18:250–255.

Edwards FA, Gibb AJ, Colquhoun D (1992) ATP receptor-mediated synaptic current in the central nervous system. Nature 359:144–147.

Edwards FA, Robertson SJ, Gibb AJ (1997) Properties of ATP receptor-mediated synaptic transmission in the rat medial habenula. Neuropharmacology 36:1253–1268.

Harden TK, Boyer JL, Nicholas RA (1995) P2Y-purinergic receptors: subtype-associated signalling responses and structure. Annu Rev Pharmacol Toxicol 35:541–579.

Illes P, Nurenberg W (1993) Neuronal ATP receptors and their mechanism of action. Trends Pharmacol Sci 14:50–54.

Khakh BS, Zhou X, Sydes J, Galligan JJ, Lester HA (2000) State-dependent cross-inhibition between transmitter gated cation channels. Nature 406:405–410.

Koizumi S, Inoue K, Koch H (1997) Inhibition by ATP of calcium oscillations in rat cultured hippocampal neurones. Br J Pharmacol 122:51–58.

Kyrozis A, Albuquerque C, Gu J, MacDermott AB (1996) Ca^{2+}-dependent inactivation of NMDA receptors: fast kinetics and high Ca^{2+} sensitivity in rat dorsal horn neurons. J Physiol (Lond) 495:449–463.

Luscher C, Nicoll RA, Malenka RC, Muller D (2000) Synaptic plasticity and dynamic modulation of the postsynaptic membrane. Nat Neurosci 3:545–550.

Lytton J, Waistline M, Hanley MR (1991) Thapsigargin inhibits the sarcoplasmic or endoplasmic reticulum Ca-ATPase family of calcium pumps. Biol Chem 266:17067–17071.

Malenka RC, Nicoll RA (1999) Long-term potentiation—a decade of progress? Science 285:1870–1874.

Mori M, Heuss C, Gahwiler BH, Gerber U (2001) Fast synaptic transmission mediated by P2X receptors in CA3 pyramidal cells of rat hippocampal slice cultures. J Physiol (Lond) 535:115–123.

Nakazawa K (1994) ATP-activated current and its interaction with acetylcholine-activated current in rat sympathetic neurons. J Neurosci 14:740–750.

Pankratov Y, Castro E, Miras-Portugal MT, Krishtal O (1998) A purinergic component of the excitatory post-synaptic current mediated by P2X receptors in the CA1 neurons of the rat hippocampus. Eur J Neurosci 10:3898–3902.

Pankratov Y, Lalo U, Castro E, Miras-Portugal MT, Krishtal O (1999) ATP receptor-mediated component of the excitatory synaptic transmission in the hippocampus. In: Progress in brain research, Vol 120 (Illes P, Zimmermann H, eds), pp 237–249. Amsterdam: Elsevier.

Pankratov Y, Lalo U, Dashkin A, Krishtal OA (2001) Heterogeneity of the functional expression of P2X3 and P2X2/3 receptors in the primary nociceptive neurons of rat. Neurochem Res 26:993–1000.

Ralevic V, Burnstock G (1998) Receptors for purines and pyrimidines. Pharmacol Rev 50:413–492.

Rosenmund C, Feltz A, Westbrook GL (1995) Calcium-dependent inactivation of synaptic NMDA receptors in hippocampal neurons. J Neurophysiol 73:427–430.

Seguela P, Haghighi A, Soghomonian J, Cooper E (1996) A novel neuronal P2X ATP receptor ion channel with wide distribution in the brain. J Neurosci 16:448–455.

Virginio C, North A, Surprenant A (1998) Calcium permeability and block at homomeric and heteromeric $P2X_2$ and $P2X_3$ receptors, and P2X receptors in rat nodose neurons. J Physiol (Lond) 510:27–35.

Zhou X, Galligan JJ (1998) Non-additive interaction between nicotinic cholinergic and P2X purine receptors in guinea-pig enteric neurons in culture. J Physiol (Lond) 513 3:685–697.

Zimmermann H (1994) Signalling via ATP in the nervous system. Trends Neurosci 17:420–426.